energy&fuels

Article

pubs.acs.org/EF

Development of Ga Salt of Molybdophosphoric Acid for Biomass Conversion to Levulinic Acid

Vijay Bhooshan Kumar, Indra Neel Pulidindi, Rahul Kumar Mishra, and Aharon Gedanken*

Bar-Ilan Institute for Nanotechnology and Advanced Materials, Department of Chemistry, Bar-Ilan University, Ramat-Gan 5290002, Israel

Supporting Information

ABSTRACT: Efficient catalytic methods for biomass conversion present a challenge for the sustainable production of fuels and chemicals. Ga salt of molydophosphoric acid (GaHPMo) is prepared using a sonochemical irradiation method. Simultaneous formation of GaHPMo and entrapment of polyoxometallate in gallium micro-/nanoparticles (Ga@HPMo) is achieved. The amount of entrapped hetropoly acid in Ga particles is estimated to be ∼3 wt %, as determined from thermogravimetric analysis (TGA) and ultraviolet−visible (UV−vis) analysis. The preparation of GaHPMo is accomplished by subjecting an ethanolic solution of polyoxometallate [molybdophosphoric acid (HPMo)] and molten Ga metal to sonication at 50 °C for 12 min. Physicochemical properties of GaHPMo are studied using X-ray diffraction, TGA, temperature-programmed desorption, differential scanning calorimetry, Fourier transform infrared spectroscopy, UV−vis spectroscopy, scanning electron microscopy, transmission electron microscopy, dynamic light scattering, and energy-dispersive X-ray spectroscopy analysis. GaHPMo was successfully used as a catalyst for the conversion of various carbohydrates (glucose, starch, and cellulose) and rice straw into levulinic acid via a hydrothermal process. Reaction conditions for obtaining an optimum yield of levulinic acid from glucose are deduced (time, 10 h; temperature, 423 K; and mole ratio of the catalyst/reactant, 1:5). The reaction products are analyzed qualitatively using nuclear magnetic resonance (^{13}C and ^{1}H) spectroscopy and quantified using high-performance liquid chromatography analysis. The maximum yield of levulinic acid obtained from glucose is 56 wt %. Apart from the major product, levulinic acid, other minor byproducts, such as formic and lactic acids, are also observed.

1. INTRODUCTION

Heterogeneous catalysis plays an important role in the world's economy and chemical industry. A total of 90% of commercial chemical products are obtained by heterogeneous catalytic processes.[1] A wide variety of chemicals for use in day-to-day life are produced in catalytic processes.[2−4] Besides applications in the production of fine chemicals, catalysts are also used in pharmaceutical, automobile, and food industries. Owing to the limited supply of non-renewable fossil energy sources (petroleum, coal, and natural gas), development of green and sustainable technologies for the conversion of biomass to biofuels and chemicals is a challenge.[5−7] Protection of the natural environment is also a key factor for building a sustainable future.[6] The design of novel catalysts is the key to most of the feasible processes for the production of alternative fuels (biodiesel, bioethanol, hydrogen, or methanol). From the "green chemistry" perspective, it is also essential to develop new catalysts and alternative processes that reduce the use of precious metals and eliminate the utilization of toxic raw materials or production of harmful byproducts, leading to a reduction in environmental contamination.

The possibility of employing biomass-derived carbohydrate as a feedstock for chemical production is being explored vigorously. Conversion of biomass into useful chemicals is one of the current trends in green chemistry.[1,3] Utilization of alternate feedstock for the production of chemicals is inevitable, owing to the uncertainty in the sustainability of fossil-based resources and the accompanying adverse effects on the environment.[8] Carbohydrate is an abundant and renewable resource obtained from biomass. Carbohydrate (glucose, sucrose, starch, and cellulose)-rich biomass is a promising feedstock for the production of chemicals (fine and platform) and biofuels. Therefore, green methods to achieve efficient and cost-effective conversion of carbohydrates are sought.

Mineral acids, such as HCl, H_2SO_4, and H_3PO_4, are the most common catalysts for the preparation of levulinic acid (LA) with high catalytic activity.[9] Such processes pose several disadvantages, such as environmental pollution and corrosion to equipment. Therefore, replacement of the mineral acids by solid acid catalysts could alleviate the associated problems. Solid super acids received attraction for their environmental benefits and absence of corrosion to equipment.[10] Moreover, solid acid catalysts can also reduce the production cost because they could be easily recycled and used several times without loss of catalytic activity. Substitution of one proton of tungstophosphoric acid (HPW) by cesium or potassium cation exerted no measurable effect on the catalytic activity.[11] Filek et al. studied the preparation and characterization and tested the catalytic properties of $GaPW_{12}O_{40}$ and $InPW_{12}O_{40}$ for the etherification of ethanol.[12] Tokarz-Sobieraj et al. described the properties of active sites in 12-tungsto- and 12-molybdophosphoric acid salts containing Al^{3+}, Ga^{3+}, and In^{3+} as counter-cations ($MePW_{12}O_{40}$ and $MePMo_{12}O_4$) using the density functional theory (DFT) theoretical modeling and examined

Received: September 19, 2016
Revised: November 7, 2016
Published: November 7, 2016

DOI: 10.1021/acs.energyfuels.6b02403
Energy Fuels XXXX, XXX, XXX−XXX

Table 1. Production of LA from Biomass Using Solid-Acid-Based Catalysts

feedstock	methodology	catalyst	yield/conversion (wt %)	reference
glucose	hydrothermal process at 1.7 MPa and variation of the Si/Ga ratio	MFI-type zeolite with different SiO_2/ Al_2O_3 ratios	yield of 29.5	24
cellulose	hydrothermal reaction at 180 °C for 3 h with 2 wt % catalyst and 2 g of cellulose	zirconium dioxide	yield of 45.8	25
glucose	autoclave sealed and purged by nitrogen gas in a stirring state at 400 rpm pressured at 1.7 MPa, with time of 8 h and temperature of 180 °C	ZRP zeolites	yield of 35	26
cotton straw (hydrolyzed sugar)	heated to 180 °C with stirring (200 rpm) for 1 h	H_2SO_4	yield of 42.6	27
microcrystalline cellulose (Avicel PH-101)	moderate temperatures (190−270 °C) to produce organic water-soluble compounds, including glucose and HMF; water-soluble compounds are further reacted with a solid acid catalyst at relatively low temperatures (160 °C) to produce LA and formic acid	zirconium phosphate catalyst (ZrP)	yield of 29	28
xylose	under hot-compressed water for 1−7 h, with three different types of gases, including helium, air, and nitrogen, were studied to consider the formation of humin and side products	alkali-treated zeolite catalysts	yield of 30	29
glucose or cellulose/starch/rice straw	hydrothermal reaction at 175 °C for 6 h	Ga@HPMo and GaHPMo	yield of 56 and 46	current study

their catalytic activity for the etherification reaction. A correlation between Brønsted acidity and catalytic activity were observed.[13] Recently, Filek et al. reported the synthesis of monocationic ($GaPW_{12}O_{40}$ and $AlPW_{12}O_{40}$) and bicationic ($CsGa_{0.5}H_{0.5}PW_{12}O_{40}$ and $CsAl_{0.5}H_{0.5}PW_{12}O_{40}$) salts of HPW for ethylene and diethyl ether production from ethanol.[14] Kimura et al. have reported the inorganic solid acids of Cs salt of 12-tungstophosphoric acid $Cs_{2.5}H_{0.5}PW_{12}O_{40}$ as being a better catalyst than H_2SO_4, $H_3PW_{12}O_{40}$ and *p*-toluenesulfonic acid.[15] Moreover, Okuhara et al. also reported the insoluble heteropoly compounds as highly active catalysts for liquid-phase reactions because of the high activity of $Cs_{2.5}$ salt. This is due to the large number of surface acid sites and its acid−base bifunctional nature, in which a cesium ion possibly increases the basicity of the heteropolyanion.[16]

Glucose is a monomeric sugar that could be obtained by the hydrolysis of starch/cellulose of plant materials.[17] A wide range of chemicals is produced from glucose.[13,14] LA,[19] γ-valerolactone,[20,21] and hydroxymethylfurfural (HMF) are examples of such chemicals. LA is prepared by treating cellulosic biomass with acid and could be obtained from a wide range of cellulosic feedstock, such as *Cicer arietinum*, cotton, *Pinus radiata*, and sugar cane bagasse.[22] Kumar et al. reported a synergistic catalytic ($ZnBr_2$−HCl) process for the production of LA from carbohydrates under microwave irradiation.[19] 1,4-Pentanediol is the hydrogenation product of LA that can be used as a monomer for polyester production.[23] Some of the recent reports on the production of LA using solid-acid-based catalysts are summarized in Table 1.

From the above reports, it is understood that solid acid catalyst forms an inexpensive and promising support material for the active metal nanoparticles in the generation of acidic sites that facilitate the conversion of biomass to LA. It is worth mentioning here that there has been no single report on the exploitation of Ga salts of heteropoly acids for biomass conversion.

A unique sonochemical approach was employed for designing the GaHPMo catalyst, which was subsequently used for the conversion of biomass to LA under hydrothermal reaction conditions. We have recently developed a methodology of sonochemical irradiation of molten metal yielding a variety of new products.[30,31] This method was used for the preparation of the Ga@HPMo catalyst. In addition, the current study presents a detailed investigation of the optimized production of LA using the solid acid catalyst in a hydrothermal reaction. The focus of the present work is to design a novel Ga-based heteropoly acid catalyst using the sonochemical method and to exploit the catalyst for the production of LA from biomass (glucose, starch, cellulose, and rice straw).

2. EXPERIMENTAL SECTION

2.1. Chemicals. Molybdophosphoric acid, $H_3PMo_{12}O_{40}{\cdot}xH_2O$ (HPMo, ACS reagent, CAS Registry Number 51429-74-4), was procured from Sigma-Aldrich. Gallium metal (99.999%) was purchased from Alfa Aeser Pvt. Ltd., Israel. Glucose, sucrose, starch (from potato), and cellulose (Avicel PH-101, 99.8%) were purchased from Sigma-Aldrich. Pretreated rice straw was provided by Professor T. H. Kim, South Korea.[32] Ethanol and isopropanol (99.7%) were purchased from Daejung Chemicals & Metals Co., South Korea. All reagents were used without further purification. Double-distilled water (DDW) was used as a solvent for the hydrothermal reactions.

2.2. Formation of Ga Salt of Polyoxometallate (GaHPMo). GaHPMo is synthesized by sonication. Solid Ga metal (70 mg, 1 mM) was melted in an ethanolic solution of HPMo (1 mM, 20 mL) in a quartz test tube (diameter of tube of 20 mm) that was dipped in a water bath at 50 °C. The titanium horn of an ultrasonic transducer [Sonics and Materials, model VCX 750, with a frequency of 20 kHz and voltage of 230 V alternating current (AC)] tip (ultrasonic tip diameter of ca. 10 mm) was dipped in the solution, and when the gallium was molten, the system was sonicated for a 12 min at 60% amplitude. A greenish gray suspension (Figure S1 of the Supporting Information) was obtained. The supernatant contained GaHPMo, which was separated from the precipitate (Ga@HPMo, HPMo encapsulated in Ga spheres) upon centrifugation. The supernatant was subjected to rotary evaporation (30 min) to evaporate ethanol. The resulting solid material, GaHPMo, was collected and dried in an antichamber of the glovebox under a N_2 atmosphere. GaHPMo, thus prepared, was characterized by a variety of physicochemical methods to understand the details of composition and properties of the material, and this forms the subject of discussion in the subsequent section.

2.3. Characterization. GaHPMo is analyzed by X-ray diffraction (XRD) measurements with a Bruker D8 Advance X-ray diffractometer using Cu Kα radiation operating at 40 kV/30 mA with a 0.02 step size and a 1 s step. The concentration of gallium and molybdenum in GaHPMo is measured by inductively coupled plasma optical emission spectrometry (ICP−OES). A typical analyte for ICP−OES analysis was prepared by the dissolution of an aliquot of GaHPMo (10 mg) in a mixture of 0.5 M HNO_3 (30 mL) and 0.5 M HCl (30 mL) at 75 °C for 3 h under stirring. Subsequently, most of the acid was evaporated, and distilled water is added and evaporated again. This process was repeated 3 times to reduce the acid concentration, and then the analyte is subjected to ICP−OES analysis. High-resolution scanning electron microscopy (HRSEM) images of the analyte, for probing the

DOI: 10.1021/acs.energyfuels.6b02403
Energy Fuels XXXX, XXX, XXX−XXX

surface morphology, are obtained with a FEI Megallon 400L microscope, operated at 20 kV. Elemental analysis and elemental mapping are performed by HRSEM energy-dispersive X-ray spectroscopy (EDS). Transmission electron microscopy (TEM) is performed for the particle size distribution of the material with a Tecnai G2, FEI high-contrast/cryo-TEM, Hillsboro, OR, equipped with bottom charge-coupled device (CCD) camera 1Kx1K. Samples for TEM analysis are prepared from a suspension of the particles of GaHPMo in isopropanol, using a sonication bath. Two droplets of the analyte are applied to a TEM carbon-coated copper grid and dried in a covered Petri dish. High-resolution transmission electron microscopy (HRTEM) analysis is performed using a JEOL 2100 microscope operated at 200 keV. Ultraviolet−visible (UV−vis) spectra of GaHPMo and Ga@HPMo were measured using a Cary 100 spectrophotometer (Varian), operated by Lab Sphere software. DSC analysis is performed using a NETZSCH instrument model 200 F3MAIA using liquid nitrogen for cooling the system. Thermogravimetric analysis (TGA) is performed using the Mettler Toledo model TGA/SDTA851^e at a scan rate of 10 K/min up to 800 °C in the N_2 gas flow. X-ray photoelectron spectroscopy (XPS) analyses of samples are performed using an ESCALAB 250 spectrometer with a monochromatic X-ray source with Al Kα excitation (1486.6 eV). Binding energy calibration is based on the signal corresponding to a C 1s signal at 285 eV. Dynamic light scattering (DLS) measurements for particle size distribution studies are performed on ZetaSizer Nano-ZS (Malvern Instruments, Ltd., Worcestershire, U.K.).

2.4. Catalytic Activity of GaHPMo. GaHPMo was used as a catalyst for the conversion of a variety of carbohydrates (glucose, sucrose, starch, and cellulose) and widely available biomass (rice straw) to LA. A typical catalytic test reaction comprises of taking a known amount of carbohydrate (0.5−1 g) and catalyst (0.05−0.1 g) and 15 mL of distilled water in a Teflon-lined stainless-steel autoclave. The autoclave is procured from stainless-steel autoclaves with a polytetrafluoroethylene (PTFE) hydrothermal synthesis reactor (MH-25) liner made in China. Pictorial representation of the autoclave used for the catalytic reactions is provided in Figure S2 of the Supporting Information. Hydrothermal treatment was carried out for 3−12 h in the temperature range between 393 and 448 K. The reaction conditions, such as the reaction time, temperature, weight/weight percent ratio of the catalyst/reactant, are varied to improve the LA yield from carbohydrates. The unreacted substrate, in the case of rice straw, is separated from the reaction products by centrifugation at 9000 rpm at 10 °C for 20 min. The reaction products obtained in each case are analyzed qualitatively by ^{1}H and ^{13}C nuclear magnetic resonance (NMR) spectroscopy on a Bruker Avance DPX 300/400 instrument using D_2O as a solvent.[19] The amount of LA and other byproducts (formic and lactic acids) of the reaction are quantified using high-performance liquid chromatography (HPLC) analysis on a Merck-Hitachi LaChrom System L-7000 instrument equipped with a L-7455 diode array detector (DAD) and a Schambeck SFD RI 2000 refractive index (RI) detector Bad Honnef, Germany. Reaction products were analyzed using a 300 × 7.8 mm REZEX-ROA ion-exclusion chromatography column, Phenomenex, Torrance, CA.

3. RESULTS AND DISCUSSION

3.1. UV−Vis Analysis. The differences in the absorption of the chemical species present in the supernatant and precipitate formed during the sonochemical irradiation of aqueous solution of HPMo and Ga metal were probed using UV−vis spectroscopy. UV−vis spectra of the aqueous solutions of HPMo, GaHPMo, and Ga@HPMo are shown in Figure 1.

UV−vis spectrum of aqueous solution of pure HPMo is different from that of either GaHPMo or Ga@HPMo, indicating the formation of new products. In the case of pure HPMo, a single absorption band at 215 nm, typical of the charge transfer from O−Mo (electron transitions within Mo−O−Mo tricenter bonds of the polyoxoanionic framework), is observed.[33] This is typical of the Keggin-type polyanion

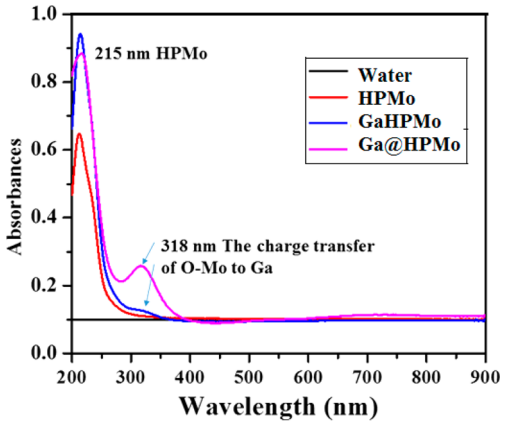

Figure 1. UV−vis spectra of HPMo, GaHPMo, and Ga@HPMo.

structure present in HPMo. This signal at 215 nm is retained in the case of both GaHPMo and Ga@HPMo. Thus, sonication has not resulted in the degradation of the Keggin structure, and the original polyanion structure, $[PMo_{12}O_{40}]^{3-}$, is retained after the sonochemical irradiation. In addition, a new absorption band appeared at 318 nm in both systems GaHPMo and Ga@HPMo. The intensity of the absorption (0.12 in GaHPMo and 0.27 in Ga@HPMo) band at 318 nm is low in the case of GaHPMo (the supernatant) and pronounced in the case of Ga@HPMo (the precipitate). This new absorption band at 318 nm is attributed to the charge transfer from O^{2-} to Ga^{3+}. Similar phenomena were observed in $Gd_3Ga_5O_{12}$.[34] The appearance of the new band at 318 nm is indicative of the presence of Ga species in the GaHPMo system and indicates the interaction of Ga species with the O^{2-} species in the Keggin-type polyanion structure. Such interactions could be due to the encapsulation of $[PMo_{12}O_{40}]^{3-}$ polyanions in the Ga spheres.

The nature of bonding between various species in HPMo systems is probed further using Fourier transform infrared spectroscopy (FTIR) analysis. The FTIR spectrum of HPMo is characterized by the four consecutive bands in the range of 700−1100 cm^{-1} typical of four different kinds of Mo−O bonds present in the Keggin-type structure. For clarity, the spectral region between 200 and 1200 cm^{-1} is presented separately in Figure 2B. In the case of HPMo, the peaks at 1065, 957, 877, and 770 cm^{-1} are attributed to the stretching modes of P−O, Mo = O, Mo−O_e−Mo, and Mo−O_c−Mo, respectively.[35,36] Even though the four consecutive absorption bands typical of the Keggin structure are retained in the case of Ga-modified polyoxometallates, a shift toward a lower wavenumber (∼10 cm^{-1}) in these bands, especially for Mo−O_c−Mo stretching, is observed. Such a shift is more pronounced in the case of Ga@HPMo, which is characteristic of the interaction between Ga^{3+} and O^{2-} (corner-shared oxygen of Mo−O_c−Mo) (Figure 2B). This observation is in concurrence with the UV−vis absorption studies (Figure 1), where an intense absorption band appeared at 318 nm, which is attributed to the charge transfer phenomena between O^{2-} of polyoxometallate and Ga^{3+} in the case of Ga@HPMo. The vibrations of OH in the range of 3000−3600 cm^{-1} and δ(OH) in the range of 1600−1650 cm^{-1} were assigned to water molecules, antisymmetric stretching in the case of pure HPMo. These signals are almost absent in the case of GaHPMo and Ga@HPMo because these systems were dried prior to FTIR analysis.

DOI: 10.1021/acs.energyfuels.6b02403
Energy Fuels XXXX, XXX, XXX−XXX

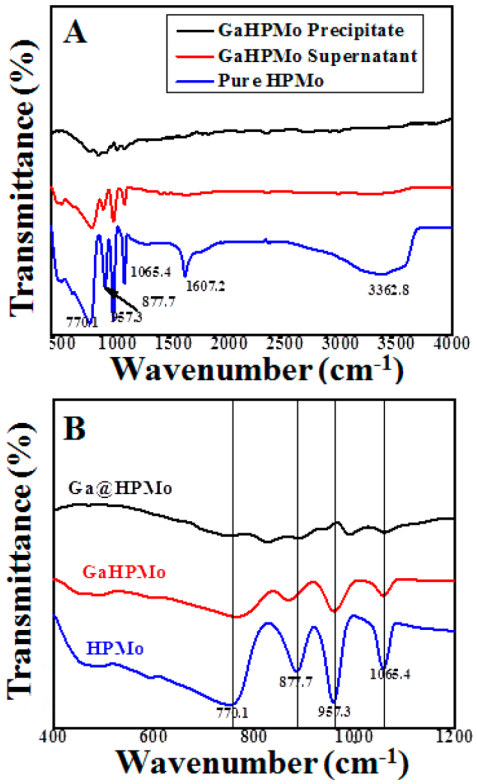

Figure 2. FTIR spectra of (A) HPMo, GaHPMo (supernatant), and Ga@HPMo (precipitate) and (B) magnified spectra of panel A in the range of 400−1200 cm^{-1}.

XRD patterns of pure HPMo, GaHPMo, and Ga@HPMo were shown in Figure S3 of the Supporting Information. As-prepared GaHPMo is amorphous with broad signals relative to either pure HPMo or GaHPMo materials. This could be due to the encapsulation of the polyoxometallate (HPMo) in molten/amorphous Ga nanoparticles. On the contrary, an intense new signal is observed in the case of GaHPMo, which was absent in the case of pure HPMo. This could be due to the presence of hydrated Ga species in the polyanion structure, $[PMoGa(OH)_2]^{2-}$. Moreover, the formation of such acidic sites is more feasible in the case of Ga salt of PMo rather than Al or In salts of HPMo. Free energy of proton formation, $\Delta G(H^+)$, is the least for GaPMo (188.3 kJ/mol) compared to either InPMo (198 kJ/mol) or AlPMo (207.4 kJ/mol).[13]

To investigate the thermal properties of metallic Ga, HPMo, GaHPMo, and Ga@HPMo, differential scanning calorimetry (DSC) analysis is carried out, and the DSC traces are shown in Figure S4a of the Supporting Information. In the case of GaHPMo, the broad endothermic peak in the range of 90−120 °C could be attributed to the removal of the water of hydration.[37] This is further supported by the TGA curve (Figure S4b of the Supporting Information), indicating ∼5 wt % loss in the temperature range of 100−150 °C. In the case of GaHPMo, the endothermic peak typical of gallium melting is not observed. This result indicates that most Ga reacted, forming the Ga salt of HPMo, $[PMoO_{40}{\cdot}Ga(OH)_2]^{2-}$. Both HPMo and Ga salt of HPMo yielded a similar DSC response with two broad endothermic peaks. On the contrary, in Ga@HPMo features typical of metallic Ga are observed, indicating the encapsulation of HPMo in Ga particles. A sharp endotherm at 28 °C in the case of Ga metal and Ga@HPMo is characteristic of melting of Ga.

The particle size distribution of GaHPMo and Ga@HPMo is measured using dynamic light scattering (DLS). A small portion of the dried samples is suspended in isopropanol using a sonication bath prior to the measurement. Three consecutive measurements (Figure 3A) showed that the particles of GaHPMo are in the size range of 100−200 nm with a narrow particle size distribution. On the contrary, Ga@HPMo particles are larger in size (150−400 nm) and also the particle size distribution is broad (Figure 3B).

Surface morphology of the dried samples of GaHPMo and Ga@HPMo is investigated using scanning electron microscopy

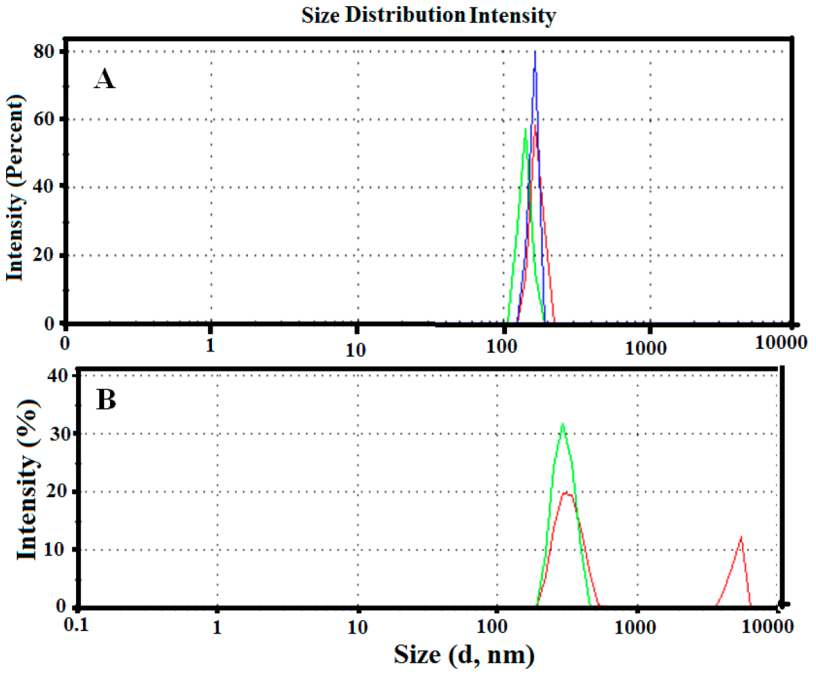

Figure 3. Particle size distribution of (A) GaHPMo and (B) Ga@HPMo from DLS analysis.

DOI: 10.1021/acs.energyfuels.6b02403
Energy Fuels XXXX, XXX, XXX−XXX

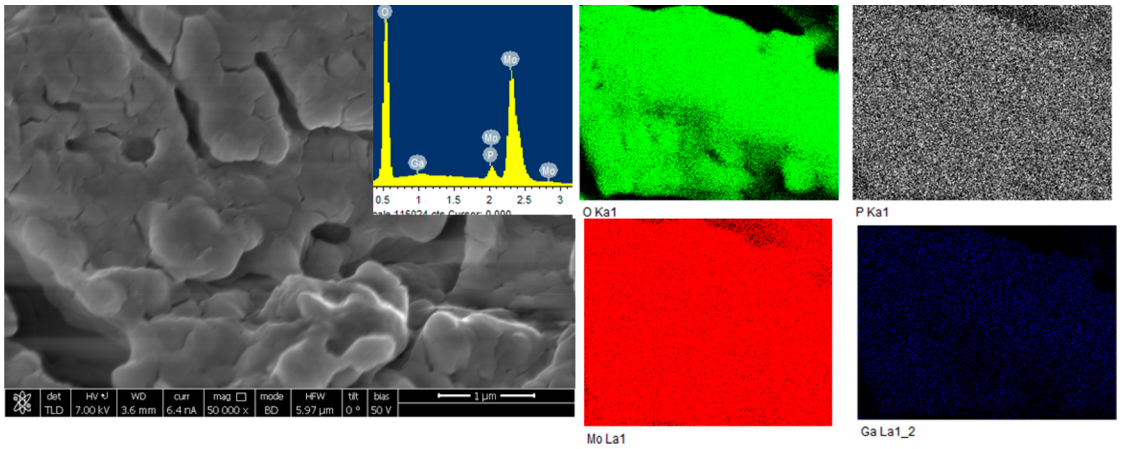

Figure 4. SEM images with elemental mapping of GaHPMo.

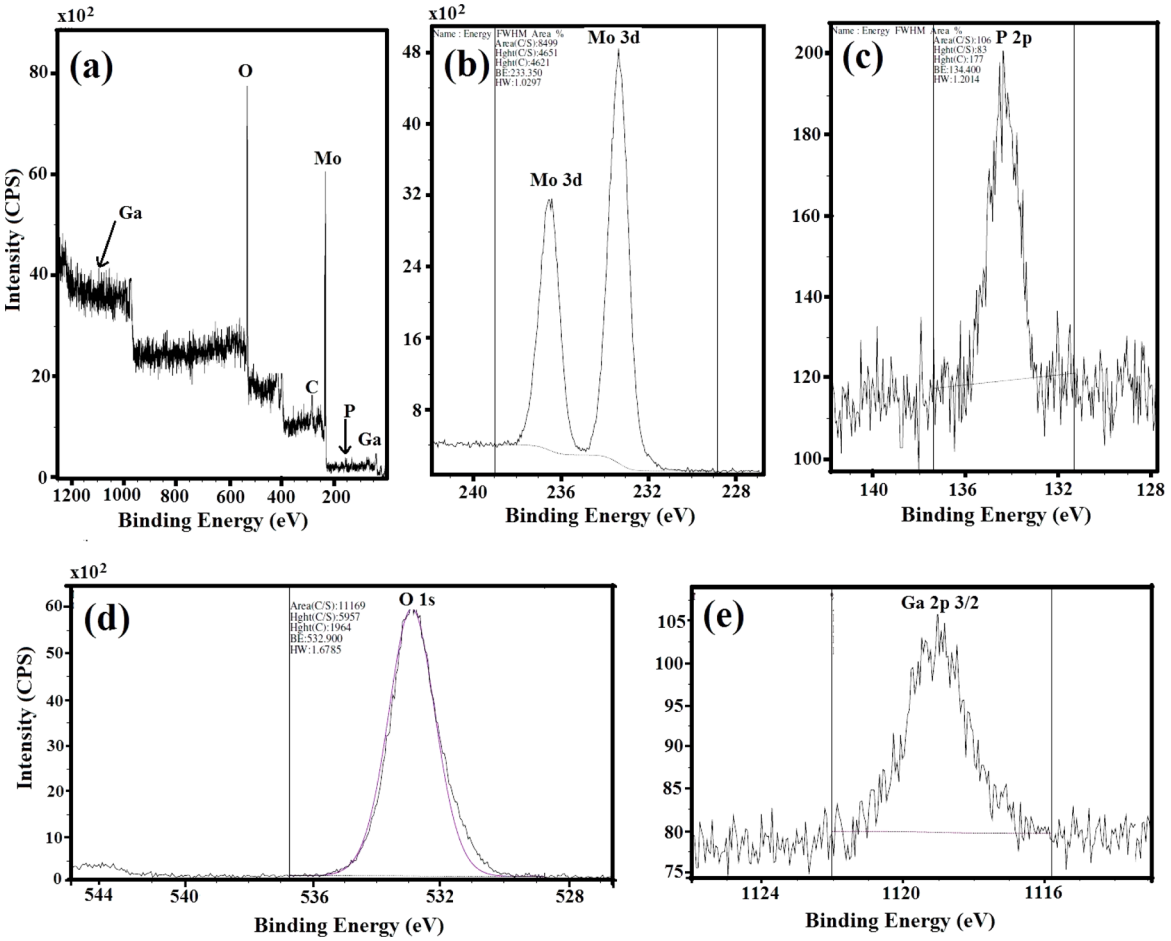

Figure 5. (a) Full XPS spectrum of Ga@HPMo, (b) XPS spectrum of Mo 3d, (c) XPS spectrum of P 2p, (d) XPS spectrum of O 1s, and (e) XPS spectrum of Ga 2p.

(SEM). A typical SEM image of GaHPMo and the corresponding EDS spectra as well as the elemental (Mo, Ga, P, and O) mapping are shown in Figure 4. The distribution of Ga metal is uniform throughout the material, especially the locations of oxygen, indicating the site of Ga^{3+} species to be close to O^{2-} species. The bigger particles are compact and composed of several nanoparticles, suggesting that synthesized GaHPMo is an agglomerate of nanoparticles. A comparison of the surface morphology and elemental composition of GaHPMo and Ga@HPMo is provided in Figure S5 of the Supporting Information. To know the exact size and shape of GaHPMo and Ga@HPMo analytes, TEM analysis was carried out. Well-dispersed, spherical GaHPMo particles with a size in the range of 30−70 nm were observed (Figure S6b of the Supporting Information). Spherical Ga@HPMo particles are larger in size (40−200 nm) owing to aggregation (Figure S6a of the Supporting Information). The result from TEM analysis is in agreement with the DLS analysis (Figure 3).

The valence states and nature of the elements present on the surface of the Ga@HPMo particles were investigated by XPS

DOI: 10.1021/acs.energyfuels.6b02403
Energy Fuels XXXX, XXX, XXX−XXX

analysis. Figure 5 show the XPS spectra of the Ga@HPMo catalyst. The characteristic peaks corresponding to O 1s (532.900 eV), Ga 2p (1118.612 eV), Mo 2p (233.350), P 2p (134.400 eV), and Ga 3d (20.188 eV) were observed in the XPS spectra. In detail, a strong single peak for Ga 2p at 1118.523 eV and 3d at 20.320 eV were assigned to Ga^{3+}.[18] Note that XPS will analyze only the surface properties of materials (less than 3 nm depth from the surface). The surface of Ga particles might be covered with Ga_2O_3 or GaO(OH) in the form of Ga^{3+}, but the percentage was very low (less than 0.1%).

The amount of Ga in GaHPMo were determined in the following manner: a 14 mg sample of GaHPMo was immersed in 0.5 M HNO_3 for about 1 h at 60 °C to dissolve the particles. The water was added after evaporation, and this process was continued 3 times. The final volume of the solution was brought to 20 mL. The concentration of Ga determined by ICP−OES was 142.1 mg/L; therefore, the total weight of Ga in the sample was 1.42 mg. This corresponds to ca. 10.28 wt % of Ga content in 14 mg GaHPMo sample. In addition, ICP analysis was carried out for the used catalyst after the reaction and the same Ga concentration (~138 mg/L) in GaHPMo was obtained. Moreover, the leaching of Ga into the hydrolysate was also studied, and a very low concentration of Ga was found (12 ppm).

3.2. Evaluation of the Catalytic Activity of GaHPMo for the Production of LA. *3.2.1. Effect of the Type of Catalyst on the Conversion of Glucose.* The hydrothermal reaction of glucose (0.5 g) in 15 mL of water is conducted using different catalysts, HPMo, GaHPMo, and Ga@HPMo, for 12 h at 150 °C. When the reaction is carried out with metallic Ga or in the absence of a catalyst, glucose conversion is not observed (Figure 6). The peaks of the reactant glucose

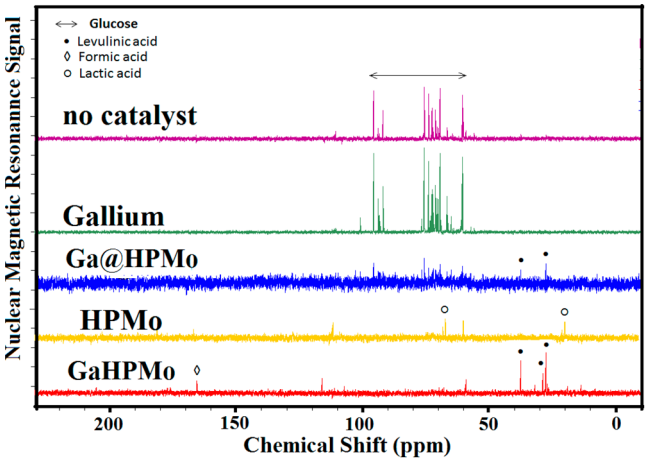

Figure 6. ^{13}C NMR spectra of the reaction products obtained from the hydrothermal reaction (12 h at 150 °C) of glucose (0.5 g of glucose in 15 mL of H_2O) with different catalysts (0.1 g).

[60.3 ppm (C6), 69.2 ppm (C4), 72.4 ppm (C2), 73.7 ppm (C3), 75.3 ppm (C5), 92 ppm (C1α), and 95.3 ppm (C1β)] remained as is (Figure 6). With pure HPMo as a catalyst, glucose is converted to lactic acid. In the case of GaHPMo, complete conversion of glucose to LA of 27.9 ppm (C1), 29.1 ppm (C2), and 37.7 ppm (C3) and formic acid (166 ppm) is observed. Under identical reaction conditions with Ga@HPMo, even though the desired product LA is formed, the conversion of glucose is not complete. Thus, GaHPMo is the selective and active catalyst for the conversion of glucose to LA. Further studies (optimization of the reaction temperature and the ratio of catalyst/reactant) for obtaining the maximum yield of LA were carried out using the GaHPMo catalyst. The details of the conversion of glucose and the distribution of the products in the hydrolyzate as a function of the type of catalyst are summarized in Table 2.

Table 2. Effect of the Type of Catalyst on the Conversion of Glucose[a]

	reactant	reaction product		
type of catalyst	glocose	glucose	LA[b]	FA[c]
no catalyst	+[d]	+	−[e]	−
gallium	+	+	−	−
Ga@HPMo	+	+	+	+
HPMo	+	+	+	+
GaHPMo	+	−	+	+

[a]Amount of glucose, 0.5 g; catalyst, 0.1 g; and temperature, 150 °C. [b]LA = levulinic acid. [c]FA = formic acid. [d]+ = present. [e]− = absent.

3.2.2. Effect of the Weight/Weight Percent Ratio of Catalyst/Reactant on the Conversion and Selectivity. The ratio (wt/wt %) of GaHPMo and glucose is varied as 1:10, 1:7, and 1:5. The hydrothermal reaction is carried out for 12 h at 150 °C. Complete conversion of glucose to LA and formic acid is observed when the ratio is 1:5. In this particular case, the signals characteristic of glucose are absent and signals typical of LA and formic acid are present (Figure S7 of the Supporting Information). When the ratio of GaHPMo/glucose is either 1:10 or 1:7, even though the glucose conversion is selective toward LA and formic acid, the glucose conversion is not complete, as evident from the signals of unreacted glucose in the reaction product. Thus, the optimum ratio of catalyst/substrate is 1:5. The details of the conversion of glucose and the distribution of the products in the hydrolyzate as a function of the effect of the weight/weight percent ratio of catalyst/reactant are summarized in Table 3.

Table 3. Effect of the Weight/Weight Percent Ratio of Catalyst/Reactant on the Conversion and Selectivity[a]

	reactant	reaction product		
weight/weight percent	glocose	glucose	LA[b]	FA[c]
1:10	+[d]	+	−[e]	−
1:7	+	+	+	+
1:5	+	−	+	+

[a]Type of glucose, GaHPMo; catalyst, 0.1 g; and temperature, 150 °C. [b]LA = levulinic acid. [c]FA = formic acid. [d]+ = present. [e]− = absent.

3.2.3. Effect of the Hydrothermal Reaction Time on the Conversion of Glucose to LA. After the most appropriate catalyst and optimal ratio of catalyst/substrate were identified, the hydrothermal reaction was conducted at different reaction times (3, 6, and 10 h) with a 1:5 ratio (wt/wt %) of GaHPMo and glucose at 150 °C.

The reaction products in each case were analyzed by ^{13}C NMR, and the spectra are shown in Figure 6. Complete conversion of glucose to LA is achieved when the hydrothermal reaction is performed for 10 h, as evident from the absence of glucose signals (Figure 7). The product contains LA and formic acid, as expected. When the reaction is carried out for 3 h, no

DOI: 10.1021/acs.energyfuels.6b02403
Energy Fuels XXXX, XXX, XXX−XXX

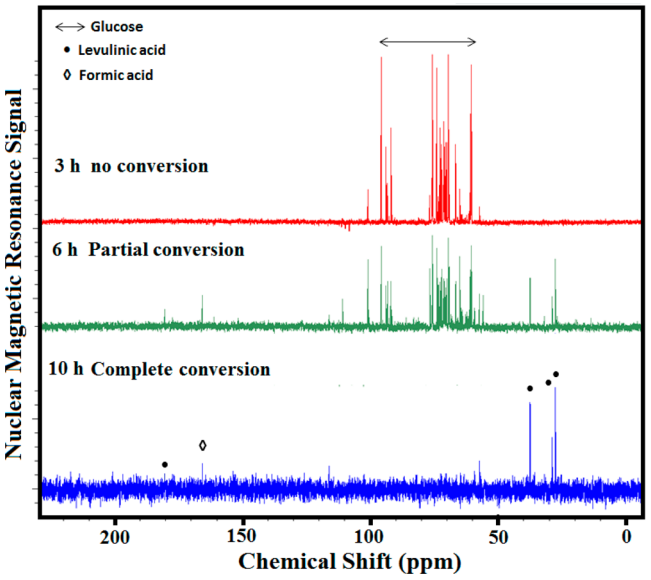

Figure 7. ^{13}C NMR spectra of the products obtained by the hydrothermal reaction of glucose with GaHPMo catalysts for different reaction times (3, 6, and 10 h).

conversion of glucose is observed and only partial conversion of glucose to LA is observed in the case of the reaction product collected at 6 h (Figure 7). The detailed conversion of glucose and the product distribution as a function of the reaction time are shown in Table 4.

Table 4. Effect of the Hydrothermal Reaction Time on the Conversion of Glucose to LA

	reactant	reaction product		
time of reaction (h)	glucose	glucose	LA[a]	FA[b]
3	+[c]	+	–[d]	–
6	+	+	+	+
10	+	–	+	+

[a]LA = levulinic acid. [b]FA = formic acid. [c]+ = present. [d]– = absent.

3.2.4. Effect of the Reaction Temperature on the Conversion of Glucose. After we learned that a minimum of 10 h of reaction time is required for the complete conversion of glucose, the temperature of the hydrothermal reaction is systematically varied from 120 to 170 °C. The ratio of HPMo/glucose is 1:5, and the reaction time is 10 h. The ^{13}C NMR spectra of the reaction products are shown in Figure S8 of the Supporting Information. Complete conversion of glucose to LA is achieved when the hydrothermal reaction temperature is 150 °C, as evident from the complete absence of signals typical of glucose. In the case of the reaction product of the reaction carried out at 120 °C, glucose conversion is incomplete and signals typical of glucose are observed along with the peaks of reaction products, LA and formic acid. The detailed conversion of glucose and the hydrolyzate product distribution as a function of the reaction temperature are shown in Table 5.

3.3. Determination of the Yield of LA from Glucose under Optimal Hydrothermal Reaction Conditions Using HPLC Analysis. Quantification of LA and formic acid in the reaction product obtained under optimal hydrothermal reaction conditions (T = 150 °C, t = 10 h, and GaHPMo/glucose = 1:5, wt/wt) was determined by HPLC. In

Table 5. Effect of the Reaction Temperature on the Conversion of Glucose

	reactant	reaction product		
reaction temperature (°C)	glucose	glucose	LA[a]	FA[b]
120	+[c]	+	–[d]	–
150	+	–	+	+
170	+	–	+	+

[a]LA = levulinic acid. [b]FA = formic acid. [c]+ = present. [d]– = absent.

concurrence with the ^{13}C NMR analysis of the reaction product obtained by the hydrothermal reaction of glucose in the presence of GaHPMo at 10 h, the highest LA yield of 56 wt % and complete conversion of glucose were shown. A comparison of the chemical composition of the reaction production obtained at 6 and 10 h of the hydrothermal reaction of glucose is shown in the histogram in Figure 8.

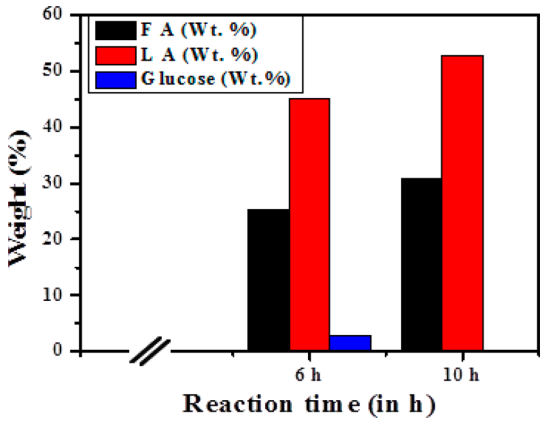

Figure 8. Quantification of LA, formic acid, and glucose by HPLC in the hydrolyzate obtained from glucose under optimal reaction conditions (LA, levulinic acid; FA, formic acid).

3.4. Conversion of Biomass to LA. The vital stages in the conversion of biomass to LA were shown in Scheme 1.

Scheme 1. Schematic Representation of the Possible Steps Involved in the Conversion of Biomass to LA

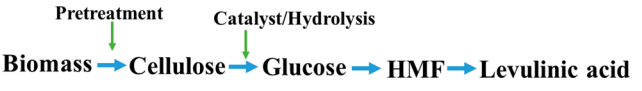

The developed methodology for the catalytic conversion of glucose to LA was further extended to other carbohydrate feedstock (starch, cellulose, and rice straw). The ^{13}C NMR spectra of the reaction products obtained from rice straw, cellulose, and starch feedstock, upon subjecting them to the hydrothermal reaction under the optimal conditions for glucose conversion, are shown in Figure 9.

In addition to the desired product, LA, the hydrolyzate obtained from pretreated rice straw, cellulose, and starch also contained glucose, as evident from the peaks in the range of 60–100 ppm. The results show the potential of GaHPMo catalyst for the conversion of biomass to LA. Scheme 2 depicts the reaction pathway of the formation of LA from glucose and biomass (rice straw, cellulose, and starch). This method is cost-effect for the production of LA, from biomass. The method can be used at the industrial level for the production of LA and

DOI: 10.1021/acs.energyfuels.6b02403
Energy Fuels XXXX, XXX, XXX–XXX

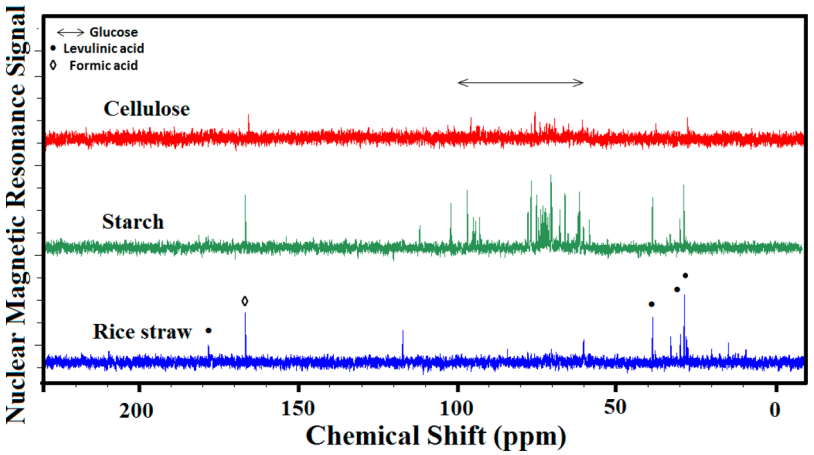

Figure 9. ^{13}C NMR spectra of the product obtained from rice straw, cellulose, and starch (10 h at 150 °C) with a different type of catalyst.

Scheme 2. Possible Reaction Mechanism for the Production of LA from Rice Straw or Glucose

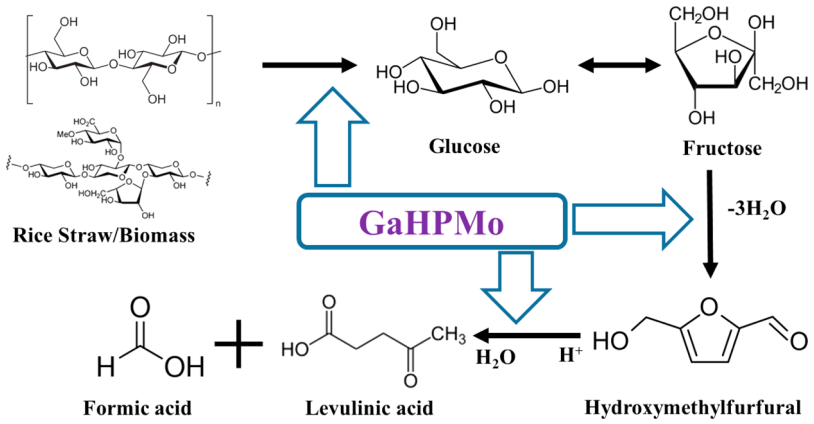

other fine chemicals using diverse cellulose-containing waste biomass, such as agricultural wastes, kitchen wastes, paper mill sludge, and cellulose fines from papermaking, as starting materials. This method indicates that the LA production cost could fall as low as $0.07/lb depending on the scale of the operation.

4. CONCLUSION

Ga salt of molybdophosphoric acid, GaHPMo, was found to be an active and selective catalyst for the conversion of biomass to LA. A LA yield of 56 wt % was achieved under optimal hydrothermal reaction conditions (T = 150 °C, t = 10 h, and GaHPMo/glucose ratio of 1:5). Thus, GaHPMo is a possible alternative to the conventional mineral acids used for the production of LA from biomass. GaHPMo exhibited superior catalytic performance in terms of activity for glucose conversion and selectivity for LA production relative to the parent HPMo. The new method for the synthesis of the keto acid (LA) is particularly important because it constitutes a key starting material for generating diesel range chemicals.

■ ASSOCIATED CONTENT

Supporting Information

The Supporting Information is available free of charge on the ACS Publications website at DOI: 10.1021/acs.energyfuels.6b02403.

Details of ^{13}C NMR spectra of certain compounds and SEM, EDS, and XRD of the catalyst (PDF)

■ AUTHOR INFORMATION

Corresponding Author

*Telephone: 972-3-5318-315. Fax: 972-3-73804053. E-mail: gedanken@mail.biu.ac.il.

ORCID

Aharon Gedanken: 0000-0002-1243-2957

Notes

The authors declare no competing financial interest.

■ ACKNOWLEDGMENTS

Aharon Gedanken thanks the Israel Ministry of Science and Technology (MoST) for Research Grant 3-99763 and the Israel Science Foundation (ISF) for supporting the research via Grant 598/12. The authors gratefully thank Professor T. H. Kim, South Korea, for providing the sample of pretreated rice straw.

■ REFERENCES

(1) Farnetti, E.; Di Monte, R.; Kašpar, J. Homogeneous and Heterogeneous Catalysis. In *Inorganic and Bio-inorganic Chemistry*; Bertini, I., Ed.; Encyclopedia of Life Support Systems (EOLSS) Publishers: Paris, France, 1999; Vol. 2, pp 50−86.

(2) Raspolli Galletti, A. M.; Antonetti, C.; Ribechini, E.; Colombini, M. P.; Nassi o Di Nasso, N.; Bonari, E. From Giant Reed to Levulinic Acid and Gamma-Valerolactone: A High Yield Catalytic Route to Valeric Biofuels. *Appl. Energy* **2013**, *102*, 157−162.

DOI: 10.1021/acs.energyfuels.6b02403
Energy Fuels XXXX, XXX, XXX−XXX

(3) Geilen, F. M.; Engendahl, B.; Harwardt, A.; Marquardt, W.; Klankermayer, J.; Leitner, W. Selective and Flexible Transformation of Biomass-Derived Platform Chemicals by a Multifunctional Catalytic System. *Angew. Chem., Int. Ed.* **2010**, *49*, 5510−5514.
(4) Cherubini, F. The Biorefinery Concept: Using Biomass instead of Oil for Producing Energy and Chemicals. *Energy Convers. Manage.* **2010**, *51*, 1412−1421.
(5) Perlatti, B.; Forim, M. R.; Zuin, V. G. Green Chemistry, Sustainable Agriculture and Processing Systems: A Brazilian Overview. *Chem. Biol. Technol. Agric* **2014**, *1*, 1−9.
(6) Axelsson, L.; Franzén, M.; Ostwald, M.; Berndes, G.; Lakshmi, G.; Ravindranath, N. H. Perspective: Jatropha Cultivation in Southern India: Assessing Farmers' Experiences. *Biofuels, Bioprod. Biorefin.* **2012**, *6*, 246−256.
(7) Sheldon, R. A. Green and Sustainable Manufacture of Chemicals from Biomass: State of the Art. *Green Chem.* **2014**, *16*, 950−963.
(8) Popp, J.; Lakner, Z.; Harangi-Rákos, M.; Fári, M. The Effect of Bioenergy Expansion: Food, Energy, and Environment. *Renewable Sustainable Energy Rev.* **2014**, *32*, 559−578.
(9) Chang, C.; MA, X.; CEN, P. Kinetics of Levulinic Acid Formation from Glucose Decomposition at High Temperature. *Chin. J. Chem. Eng.* **2006**, *14*, 708−712.
(10) Ranga Rao, G.; Rajkumar, T.; Varghese, B. Synthesis and Characterization of 1-Butyl 3-Methyl Imidazolium Phosphomolybdate Molecular Salt. *Solid State Sci.* **2009**, *11*, 36−42.
(11) Ibrahim, S. M. Catalytic Activity and Selectivity of Unsupported Dodecatungstophosphoric Acid, and Its Cesium and Potassium Salts Supported on Silica. *Mod. Res. Catal.* **2013**, *02*, 110−118.
(12) Filek, U.; Mucha, D.; Hunger, M.; Sulikowski, B. Novel Gallium and Indium Salts of the 12-Tungstophosphoric Acid: Synthesis, Characterization and Catalytic Properties. *Catal. Commun.* **2013**, *30*, 19−22.
(13) Tokarz-Sobieraj, R.; Grybos, R.; Filek, U.; Micek-Ilnicka, A.; Niemiec, P.; Kirpsza, A.; Witko, M. Generation of Acidic Sites in Al, Ga, in Salts of Molybdenum and Tungsten Keggin-Type Heteropolyacids. DFT Modeling and Catalytic Tests. *Catal. Today* **2015**, *257*, 72−79.
(14) Filek, U.; Kirpsza, A.; Micek-Ilnicka, A.; Lalik, E.; Bielański, A. Ethanol Conversion over Cesium-Doped Mono- and Bi-Cationic Aluminum and Gallium H3PW12O40 Salts. *J. Mol. Catal. A: Chem.* **2015**, *407*, 152−162.
(15) Kimura, M.; Nakato, T.; Okuhara, T. Water-Tolerant Solid Acid Catalysis of Cs2.5H0.5PW12O40 for Hydrolysis of Esters in the Presence of Excess Water. *Appl. Catal., A* **1997**, *165*, 227−240.
(16) Okuhara, T.; Nishimura, T.; Watanabe, H.; Misono, M. Insoluble Heteropoly Compounds as Highly Active Catalysts for Liquid-Phase Reactions. *J. Mol. Catal.* **1992**, *74*, 247−256.
(17) Kumar, V. B.; Pulidindi, I. N.; Gedanken, A. Selective Conversion of Starch to Glucose Using Carbon Based Solid Acid Catalyst. *Renewable Energy* **2015**, *78*, 141−145.
(18) Tzhayik, O.; Pulidindi, I. N.; Gedanken, A. Forming Nanospherical Cellulose Containers. *Ind. Eng. Chem. Res.* **2014**, *53*, 13871−13880.
(19) Kumar, V. B.; Pulidindi, I. N.; Gedanken, A. Synergistic Catalytic Effect of the ZnBr 2 − HCl System for Levulinic Acid Production Using Microwave Irradiation. *RSC Adv.* **2015**, *5*, 11043−11048.
(20) Fegyverneki, D.; Orha, L.; Láng, G.; Horváth, I. T. Gamma-Valerolactone-Based Solvents. *Tetrahedron* **2010**, *66*, 1078−1081.
(21) Horváth, I. T.; Mehdi, H.; Fábos, V.; Boda, L.; Mika, L. T. γ-Valerolactone—a Sustainable Liquid for Energy and Carbon-Based Chemicals. *Green Chem.* **2008**, *10*, 238−242.
(22) Victor, A.; Pulidindi, I. N.; Gedanken, A. Levulinic Acid Production from Cicer Arietinum, Cotton, Pinus Radiata and Sugarcane Bagasse. *RSC Adv.* **2014**, *4*, 44706−44711.
(23) Gallezot, P. Conversion of Biomass to Selected Chemical Products. *Chem. Soc. Rev.* **2012**, *41*, 1538.
(24) Fricke, R.; Kosslick, H.; Lischke, G.; Richter, M. Incorporation of Gallium into Zeolites: Syntheses, Properties and Catalytic Application. *Chem. Rev.* **2000**, *100*, 2303−2405.
(25) Joshi, S. S.; Zodge, A. D.; Pandare, K. V.; Kulkarni, B. D. Efficient Conversion of Cellulose to Levulinic Acid by Hydrothermal Treatment Using Zirconium Dioxide as a Recyclable Solid Acid Catalyst. *Ind. Eng. Chem. Res.* **2014**, *53*, 18796−18805.
(26) Zeng, W.; Cheng, D.; Zhang, H.; Chen, F.; Zhan, X. Dehydration of Glucose to Levulinic Acid over MFI-Type Zeolite in Subcritical Water at Moderate Conditions. *React. Kinet., Mech. Catal.* **2010**, *100*, 377−384.
(27) Ji, W.; Shen, Z.; Wen, Y. A Continuous Hydrothermal Saccharification Approach of Rape Straw Using Dilute Sulfuric Acid. *BioEnergy Res.* **2014**, *7*, 1392−1401.
(28) Weingarten, R.; Conner, W. C.; Huber, G. W. Production of Levulinic Acid from Cellulose by Hydrothermal Decomposition Combined with Aqueous Phase Dehydration with a Solid Acid Catalyst. *Energy Environ. Sci.* **2012**, *5*, 7559−7574.
(29) Chamnankid, B.; Ratanatawanate, C.; Faungnawakij, K. Conversion of Xylose to Levulinic Acid over Modified Acid Functions of Alkaline-Treated Zeolite Y in Hot-Compressed Water. *Chem. Eng. J.* **2014**, *258*, 341−347.
(30) Kumar, V. B.; Koltypin, Y.; Gedanken, A.; Porat, Z. Ultrasonic Cavitation of Molten Gallium in Water: Entrapment of Organic Molecules in Gallium Microspheres. *J. Mater. Chem. A* **2014**, *2*, 1309.
(31) Kumar, V. B.; Gedanken, A.; Kimmel, G.; Porat, Z. Ultrasonic Cavitation of Molten Gallium: Formation of Micro- and Nano-Spheres. *Ultrason. Sonochem.* **2014**, *21*, 1166−1173.
(32) Victor, A.; Pulidindi, I. N.; Kim, T. H.; Gedanken, A. Design of a Selective Solid Acid Catalyst for the Optimization of Glucose Production from Oryza Sativa Straw. *RSC Adv.* **2016**, *6*, 31−38.
(33) Chisholm, M. H.; Ziehm, C. J. Metal−Metal Quadruple Bonds (M = Mo or W) Supported by 4-[2-(4-Pyridinyl)ethenyl] Benzoates and Their Complexes with Tris(pentafluorophenyl)boron. *Inorg. Chem.* **2015**, *54*, 11168−11173.
(34) Matsubayashi, S.; Yakabe, F.; Kurimoto, M.; Shinagawa, K.; Saito, T.; Tsushima, T. Charge-transfer transitions of 4d- and 5d-transition elements in garnets. *J. Magn. Magn. Mater.* **1998**, *177−181*, 249−250.
(35) Lakshminarayana, G.; Nogami, M. Synthesis and Characterization of Proton Conducting Inorganic-Organic Hybrid Nanocomposite Membranes Based on tetraethoxysilane/trimethylphosphate/3-Glycidoxypropyltrimethoxysilane/heteropoly Acids. *Electrochim. Acta* **2009**, *54*, 4731−4740.
(36) Trost, M.; Schröder, S.; Duparré, A.; Risse, S.; Feigl, T.; Zeitner, U. D.; Tünnermann, A. Structured Mo/Si Multilayers for IR-Suppression in Laser-Produced EUV Light Sources. *Opt. Express* **2013**, *21*, 27852−27864.
(37) Song, Y.-F.; Abbas, H.; Ritchie, C.; McMillian, N.; Long, D.-L.; Gadegaard, N.; Cronin, L. From Polyoxometalate Building Blocks to Polymers and Materials: The Silver Connection. *J. Mater. Chem.* **2007**, *17*, 1903−1908.

DOI: 10.1021/acs.energyfuels.6b02403
Energy Fuels XXXX, XXX, XXX−XXX